



The effects of uranium speciation on the rate of U(VI) reduction by *Shewanella oneidensis* MR-1

Ling Sheng*, Jennifer Szymanowski, Jeremy B. Fein

Department of Civil Engineering and Geological Sciences, University of Notre Dame, Notre Dame, 46556 IN, USA

Received 20 July 2010; accepted in revised form 22 March 2011; available online 3 April 2011

Abstract

We measured the kinetics of U(VI) reduction by *Shewanella oneidensis* MR-1 under anaerobic conditions in the presence of variable concentrations of either EDTA or dissolved Ca. We measured both total dissolved U and U(VI) concentrations in solution as a function of time. In separate experiments, we also measured the extent of U(VI) adsorption onto *S. oneidensis* in order to quantify the thermodynamic stabilities of the important U(VI)–bacterial surface complexes. In the EDTA experiments, the rate of U(IV) production increased with increasing EDTA concentration. However, the total dissolved U concentrations remained constant and identical to the initial U concentrations during the course of the experiments for all EDTA-bearing systems. Additionally, the U(VI) reduction rate in the EDTA experiments exhibited a strong correlation to the concentration of the aqueous U⁴⁺–EDTA complex. We conclude that the U(VI) reduction rate increases with increasing EDTA concentration, likely due to U⁴⁺–EDTA aqueous complexation which removes U(IV) from the cell surface and prevents UO₂ precipitation.

In the Ca experiments, the U(VI) reduction rate decreased as Ca concentration increased. Our thermodynamic modeling results based on the U(VI) adsorption data demonstrate that U(VI) was adsorbed onto the bacterial surface in the form of a Ca–uranyl-carbonate complex in addition to a number of other Ca–free uranyl complexes. The observed U(VI) reduction rates in the presence of Ca exhibit a strong negative correlation to the concentration of the Ca–uranyl-carbonate bacterial surface complex, but a strong positive correlation to the total concentration of all the other Ca–free uranyl surface complexes. Thus, the concentration of these Ca–free uranyl surface complexes appears to control the rate of U(VI) reduction by *S. oneidensis* in the presence of dissolved Ca. Our results demonstrate that U speciation, both of U(VI) before reduction and of U(IV) after reduction, affects the reduction kinetics, and that thermodynamic modeling of the U speciation may be useful in the prediction of reduction kinetics in realistic geologic settings.

© 2011 Elsevier Ltd. All rights reserved.

1. INTRODUCTION

The oxidation state of U is one of several factors that control the mobility and fate of U in geologic settings. U(VI), in the form of the uranyl cation UO₂²⁺, is the thermodynamically stable form of U under oxic conditions. Uranyl minerals exhibit markedly higher solubilities than U(IV) phases (Langmuir, 1997), so U mobility in aerobic environments can be high. However, in anaerobic settings,

the mobility of U in the subsurface can be retarded by the reduction of soluble U(VI) species into insoluble U(IV) solid phases (Bonatti et al., 1971; Langmuir, 1997). Bacteria can reduce U(VI) to U(IV) through metabolic activity (Lovley et al., 1991, 1993; Lovley and Phillips, 1992a). Metal- or sulfate-reducing bacterial species such as *Geobacter metallireducens* (Lovley et al., 1991), *Shewanella oneidensis* (Lovley et al., 1991) and *Desulfovibrio desulfuricans* (Lovley and Phillips, 1992a) can couple the reduction of U(VI) to the oxidation of electron donors such as H₂ and lactate, and under laboratory conditions, the reduction of U(VI) to U(IV) can be both rapid and complete.

* Corresponding author. Tel.: +1 574 631 4307.
E-mail address: lsheng@nd.edu (L. Sheng).

As a result, bioreduction of U(VI) may represent a viable remediation approach for anaerobic groundwater systems contaminated with U(VI) (Lovley and Phillips, 1992b; Finneran et al., 2002; Anderson et al., 2003; Wu et al., 2007).

Although considerable research has focused on the mechanisms of U(VI) reduction by bacteria, the controls on the kinetics of the reduction process are poorly defined. Brooks et al. (2003) found that the presence of dissolved Ca could decrease the rate and extent of U(VI) reduction by *S. oneidensis*, *D. desulfuricans* and *Geobacter sulfurreducens*, likely due to the formation of the aqueous $\text{Ca}_2\text{UO}_2(\text{CO}_3)_3^0$ complex. Inhibition of U(VI) reduction rates by bacteria in the presence of dissolved Ca was also observed by Stewart et al. (2007) and by Neiss et al. (2007). Haas and Northup (2004) measured the removal rate of U(VI) by *S. oneidensis* in the presence of a range of multi-dentate organic acids, and found that the initial rates of U removal from solution decreased with increasing stability constant values for the 1:1 aqueous U(VI):ligand and U(IV):ligand complexes. Because Haas and Northup (2004) only measured total U remaining in solution and not U(VI) specifically, it remains unclear whether the observed effects were caused by ligand-retarded U(VI) reduction due to aqueous U(VI)-ligand complexation, by ligand-promoted dissolution of the solid phase UO_2 that formed on the bacteria, by ligand-promoted desorption of U^{4+} from the bacterial cell wall before UO_2 could form, or by a combination of these processes. Furthermore, Suzuki et al. (2010) demonstrated that strong complexing ligands like citrate, NTA and EDTA retard UO_2 precipitation in U(VI) bioreduction experiments by forming aqueous complexes with U(IV). Behrends and Van Cappellen (2005) found that U(VI) speciation in systems containing both bacteria and hematite nanoparticles control the pathway and kinetics of U(VI) reduction. The results of these previous studies suggest that the cell wall speciation of U may control the kinetics and extent of reductive precipitation of U(VI) by bacteria. Metal adsorption represents an important mechanism in a number of other bacterial metabolic processes as well. For example, Borrok et al. (2005b) demonstrated that the chemotactic response of *Escherichia coli* away from aqueous Ni is directly related to the concentration of Ni adsorbed onto the bacterial cell wall. We propose that the cell wall speciation of U similarly controls U(VI) reduction by bacteria.

If adsorption/desorption reactions control bacterial reductive precipitation of U(VI) to U(IV), then it is crucial to quantify the tendency of U to bind cell wall components. There have been no studies of U(IV) adsorption onto bacteria, but U(VI) adsorption onto bacteria has been examined and the thermodynamic stabilities of U(VI)-bacterial surface complexes have been quantified (Fowle et al., 2000; Haas et al., 2001; Gorman-Lewis et al., 2005). Adsorption of U(VI) onto bacterial cell walls is controlled by complexation of aqueous uranyl ions and aqueous uranyl complexes with phosphoryl and carboxyl functional groups within the bacterial cell wall (Kelly et al., 2002). Fowle et al. (2000) observed extensive adsorption of UO_2^{2+} onto the Gram-positive species *Bacillus subtilis* under low pH conditions, with increasing U(VI) adsorption with increasing pH up to approximately pH 5. Gorman-Lewis

et al. (2005) extended these observations to higher pH conditions and demonstrated that U(VI) could adsorb to the bacterial cell wall extensively, even under conditions where aqueous uranyl-carbonate, uranyl-hydroxide, and Ca-uranyl-carbonate complexes dominate the aqueous U(VI) budget. These studies use a surface complexation approach to determine stability constants for the important U(VI)-bacterial surface complexes, and these constants can serve as a basis for understanding the role of U(VI) adsorption in controlling bioreduction of U(VI).

In this study, we measured the kinetics and extent of U(VI) reduction by *S. oneidensis* MR-1 in the presence of variable concentrations of EDTA or dissolved Ca, measuring both total dissolved U and aqueous U(VI) remaining in solution in order to discern U(VI) adsorption controls from U(IV) desorption controls on the reduction kinetics. We also measured the extent of U(VI) adsorption onto *S. oneidensis* in order to quantify the thermodynamic stabilities of important U(VI)-bacterial surface complexes, and we relate those stabilities to the observed reduction kinetics.

2. EXPERIMENTAL METHODS

2.1. U(VI) reduction experiments

2.1.1. Bacteria preparation

S. oneidensis strain MR-1 was grown aerobically following procedures described previously (Fein et al., 1997; Fowle and Fein, 2000). Cells were maintained on agar plates made of trypticase soy agar with 0.5% yeast extract. Cells were first transferred from the agar plate to a tube containing 3 mL of sterile trypticase soy broth (TSB) with 0.5% yeast extract. After being incubated at 32 °C for 24 h, the cell suspension was transferred to 2 L of sterile TSB with 0.5% yeast extract and incubated at 32 °C for another 24 h.

Cells of *S. oneidensis* were harvested by centrifugation at 10,970g for 5 min. Cells were washed twice by resuspending them in 20 mL of sterile anoxic 0.1 M NaCl before the reduction experiments conducted with EDTA, or in 20 mL of sterile anoxic 30 mM NaHCO_3 before the reduction experiments with Ca. Between each wash, cells were pelleted by centrifugation at 8,100g for 5 min. After the washes, the cells were resuspended in 10 mL of sterile anoxic 0.1 M NaCl (for the EDTA experiments) or 30 mM NaHCO_3 (for the Ca experiments) in order to create a concentrated parent cell suspension that was used in the U(VI) reduction experiments.

2.1.2. U(VI) reduction experiments with EDTA

The anaerobic procedures and the general composition of the experimental medium that we used for the EDTA experiments were similar to those described previously (Balch and Wolfe, 1976; Lovley et al., 1991; Haas and Northup, 2004). The experimental medium was consisted of 5 mM NH_4Cl , 1 mM KCl, 30 mM NaHCO_3 , 40 mM Na-lactate, and vitamins solution and trace elements as per Lovley and Phillips (1988). Different amounts of EDTA disodium salt were added to the experimental medium in order to achieve final EDTA concentrations of 0.0, 0.5,

1.5, 3.0, and 5.0 mM. The pH of each experimental medium was adjusted to 7.0 using small aliquots of concentrated NaOH and/or HCl. After being heated on a hotplate, and bubbled with an 85% N₂/10% CO₂/5% H₂ gas mixture for ~15 min, the experimental medium was transferred to an anaerobic glovebox chamber, containing an atmosphere with the same 85% N₂/10% CO₂/5% H₂ gas composition. Sterile serum bottles were filled with 50 mL of experimental medium each, sealed inside the glove box, and then autoclaved outside the glovebox at 120 °C for 20 min. The pH of each medium with different EDTA concentrations was checked to be around 7.0 after being autoclaved. A uranyl acetate stock was prepared with UO₂(CH₃COO)₂·2H₂O and ultrapure 18 MΩ water and its concentration was determined by inductively coupled plasma optical emission spectroscopy (ICP-OES). The U(VI) stock solution was bubbled with the 85% N₂/10% CO₂/5% H₂ gas mixture for ~30 min, then filter-sterilized (0.2 μm) and injected into a sterile evacuated serum bottle inside the anaerobic chamber. The filter-sterilized (0.2 μm) uranyl acetate stock was added to each experimental serum bottle to achieve an initial dissolved U(VI) concentration of 0.5 mM. Two milliliters of solution was transferred from each experimental bottle to measure the initial U(VI) and total dissolved U concentrations by fluorescence spectrometry and ICP-OES, respectively.

For each concentration (0.0, 0.5, 1.5, 3.0, and 5.0 mM) of EDTA in the reduction experiments, there were three replicate sample bottles injected with 200 μL of the parent cell suspension and two cell-free control bottles with the same aqueous composition but without bacteria. The cell-free control experiments were to test if any U(VI) reduction or any loss of total U could be attributed to abiotic factors under the experimental conditions. During the experiments, all of the sample bottles and the control bottles were agitated gently and continuously at room temperature (~25 °C). To determine the initial cell density, 0.5 mL of well-mixed cell suspension was removed from three sample bottles right after injection of bacteria, 50 μL of formalin was added, and cell density was determined through direct cell counting using a Petroff-Hausser cell counting chamber. The average initial cell density in the EDTA experiments was $3.0(\pm 0.7) \times 10^7$ cells/mL.

At selected sampling times, approximately 3.5 mL of sample solution was removed under anaerobic and sterile conditions from each bottle during the initial 2.3 h of the experiment. 0.5 mL of each 3.5 mL sample was filtered through a 0.2 μm Millipore Millex PTFE filter and analyzed for dissolved U(VI) concentration by fluorescence spectrometry. A 2.5 mL aliquot of each 3.5 mL sample was filtered through a 0.2 μm Millipore Millex PTFE filter and acidified with 4.5 μL of concentrated HNO₃ (15.8 N) for total dissolved U analysis by ICP-OES. The concentration of U(IV) in the experimental systems was calculated by difference between the measured total U and dissolved U(VI) concentrations.

2.1.3. U(VI) reduction experiments with Ca

The experimental medium for the U(VI) reduction experiments with dissolved Ca consisted of 30 mM NaHCO₃ and 50 mM Na-lactate (Brooks et al., 2003). The pH

of the experimental medium was adjusted to 7.0 using small aliquots of concentrated NaOH and/or HCl. The pH adjustment did not significantly change the ionic strength of the experimental solutions. The experimental serum bottles containing 50 mL of sterile anoxic experimental medium were prepared the same way as described in the EDTA experiments part. A Ca stock solution was prepared with CaCl₂·2H₂O and ultrapure 18 MΩ water and its concentration was determined by ICP-OES. The Ca stock solution was stirred and placed inside the anaerobic chamber overnight, then filter-sterilized (0.2 μm) and injected into a sterile evacuated serum bottle inside the anaerobic chamber. Aliquots of the Ca stock solution were injected into the experimental serum bottles to achieve experimental Ca concentrations of 0.0, 0.5, 1.5, 2.5, and 5.0 mM. The pH of the medium of each Ca concentration was measured to be around pH 7.0 after addition of Ca. A initial 0.5 mM of U(VI) in each experimental bottle was achieved by following the same procedures used for the EDTA experiments. Five bottles were prepared the same way as the EDTA experiments for each concentration of Ca: 3 replicate sample bottles were injected with parent cell suspension; the other 2 bottles were cell-free controls. The determination of the initial aqueous U(VI) and total dissolved U concentrations and the average initial cell density ($3.2 \pm 0.6 \times 10^7$ cells/mL), and also the sampling procedure for the initial 5 h after cell injection were the same as the EDTA experiments. During the experimental course, all the sample bottles and the control bottles were agitated gently and continuously at room temperature (~25 °C).

2.2. U(VI) adsorption experiments

2.2.1. Bacteria preparation

S. oneidensis MR-1 was grown following the same procedures described above. The bacteria were washed following the procedure outlined in previous work (Fein et al., 1997; Fowle et al., 2000). After 48 h growth, cells of *S. oneidensis* were harvested by centrifugation at 10,970g for 5 min. Then the cells were rinsed 5 times in 0.1 M NaClO₄ with a centrifugation step of 8,100g for 5 min between each rinse. The cells were then centrifuged twice at 8,100g for 30 min, pouring off the supernatant after each centrifugation, in order to determine the wet mass of *S. oneidensis* to be used in the experiments. The wet mass is approximately 8 times the dry mass of the biomass (Borrok et al., 2005a). We assume that no U(VI) reduction occurred during these aerobic adsorption experiments, an assumption consistent with the results of Kelly et al. (2002) who conducted an EXAFS study of U(VI) adsorption onto *B. subtilis* bacterial cells.

2.2.2. U(VI) adsorption experiments

For the U(VI) adsorption experiments, an aqueous filter-sterilized uranyl acetate stock solution was prepared as described above. Aliquots of the U stock solution were added to a 0.1 M NaClO₄ electrolyte solution to form a U(VI)-electrolyte solution containing ~10 ppm (4.2×10^{-5} M) of U(VI). Before adding bacteria, this solution was sampled to determine the initial total dissolved U

concentration by ICP-OES. Then in each of two separate Teflon bottles, weighed *S. oneidensis* cells were added to the 10 ppm U(VI)-electrolyte solution to form two bacteria-U(VI)-electrolyte suspensions: one with 0.625 g (wet mass)/L of *S. oneidensis* and another with 0.25 g/L of *S. oneidensis*. The pH values of these two bacteria-U(VI)-electrolyte suspensions were adjusted to between 6 and 8 using aliquots of concentrated HNO₃ and NaOH. A number of 8 mL aliquots were taken from the parent suspensions and placed in Teflon tubes. The pH of each individual suspension was adjusted to cover the pH range of 3–9 using small volumes of HNO₃ and NaOH. After the pH adjustment, all the reaction tubes were placed on a rotating rack and gently agitated for 3 h. The final pH of each suspension was measured, and each suspension was then filtered through a 0.2- μ m Millipore Millex PTFE filter and acidified with concentrated HNO₃ for ICP-OES analysis. The concentration of the adsorbed U was calculated by difference between the measured initial and final aqueous U(VI) concentrations.

2.3. Analytical methods

2.3.1. Total dissolved U analysis by ICP-OES

A Perkin-Elmer Optima 2000DV ICP-OES system was used to determine total dissolved U in solution. Matrix-matched blanks and standards covering the probable range of U in solution were prepared. The standards including the blank were re-analyzed after running every 30–40 samples in order to check machine drift. Analytical uncertainty was approximately $\pm 2\%$, as determined by repeat analyses of an aqueous U standard, and the operational detection limit for U was determined to be approximately 60 ppb.

2.3.2. Dissolved U(VI) analysis by fluorescence spectrometry

A PTI Quantmaster QM-4 spectrofluorometer was used to measure the phosphorescence decay of U(VI) in order to determine the concentration of U(VI) in solution, following the general approach and principles described in previous studies (Gorby and Lovley, 1992; Brina and Miller, 1992). The spectrofluorometer system uses a xenon flash lamp as an excitation source and exhibits a linear dynamic range for aqueous U(VI) concentrations from 0.05 mM to 1.5 mM. The spectrofluorometer measures phosphorescence decay by recording the change in intensity of the phosphorescence signal emitted by excited U(VI) atoms in the sample as a function of time. UO₂²⁺ complexing agents are added to aqueous samples to prevent the uranyl ion from quenching after excitation (Sill and Peterson, 1947). Each sample (0.5 mL) was filtered, acidified with 0.25 mL of 12.1 N HCl, and diluted 200 times with ultrapure 18 M Ω water. 1.5 mL of Uraplex (the complexing agent) was then added to 1 mL of diluted sample and the solution was analyzed immediately on the spectrofluorometer, using an excitation wavelength of 420 nm, an emission wavelength of 515 nm and slit width of 17 nm. Matrix-matched blanks and standards covering the probable range of U(VI) in solution were measured to construct a calibration curve and to quantify the U(VI) concentrations in the samples. Analytical uncertainty was approximately $\pm 4.5\%$, as determined by repeat

analyses of an aqueous U(VI) standard, and the detection limit for U(VI) under these analytical conditions was approximately 0.05 mM.

3. RESULTS

3.1. Results of U(VI) reduction experiments with EDTA

Fig. 1 illustrates the results of U(VI) reduction by *S. oneidensis* MR-1 in the presence and absence of EDTA, depicting the measured concentrations of total dissolved U and aqueous U(VI) as a function of time in Fig. 1a and b, respectively. There was no measurable loss of total dissolved U or aqueous U(VI) in the cell-free control experiments (data not shown), indicating no significant U(VI) reduction or adsorption onto the experimental apparatus under the experimental conditions. In the experiments without EDTA, the concentration of total dissolved U decreased steadily from an initial concentration of 0.52 mM to 0.45 mM after 2.3 h (Fig. 1a). The addition of EDTA to the system caused the total dissolved U concentrations to remain unchanged over the course of the experiment for each of the EDTA concentrations studied (Fig. 1a). Additionally, all of the experiments that contained EDTA exhibited respectively clear solutions with no visible black U(IV)O₂ precipitate. Conversely, a black

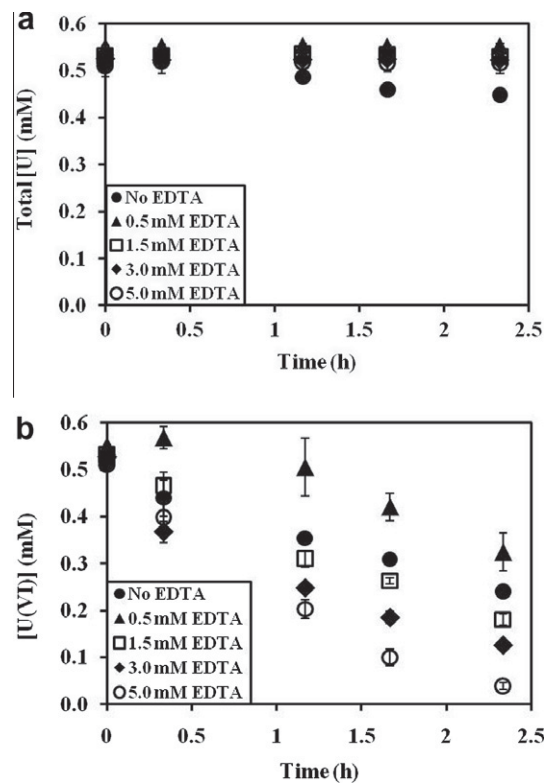


Fig. 1. The concentrations of (a) total dissolved U and (b) dissolved U(VI) remaining in solution in the presence of different concentrations of EDTA (0.0, 0.5, 1.5, 3.0, and 5.0 mM) as a function of time. Symbols represent the average of triplicate experiments, and the error bars represent the associated standard deviation (1σ) of each value.

U(IV)O₂ precipitate formed in the system that did not contain EDTA. These results are consistent with previous studies such as those by Haas and Northup (2004) and Suzuki et al. (2010).

In contrast to the total dissolved U concentrations, the concentration of U(VI) in solution decreased steadily over the course of the 2.3 h experiments for all EDTA concentrations studied (Fig. 1b). In the system without EDTA, the U(VI) concentrations decreased from 0.52 mM to 0.24 mM during the experiment. The total dissolved U concentrations were significantly higher than the U(VI) concentrations at each sampling time, suggesting that some of the U(IV) that was produced during the experiment passed through the filtration membrane and contributed to the total dissolved U concentration. The U(IV) that passed through the filter was likely in the form of UO₂ particles in the EDTA-free experiments and in the form of the aqueous EDTA–U(IV) complex in the EDTA-bearing systems. The U(VI) concentration profiles are direct measurements of the extent of U(VI) reduction and are unaffected by the presence of U(IV) in the samples, and these values alone were used to determine U(VI) reduction rates. Despite the presence of U(IV) species in the experimental samples, the total dissolved U measurements can still be used qualitatively to constrain reduction mechanisms. In general, the presence of EDTA yielded a faster rate of U(VI) reduction, with decreasing U(VI) concentrations at a given sampling time with increasing EDTA concentration. For example, after 2.3 h, the 0, 3, and 5 mM EDTA experiments contained 0.24, 0.13, and 0.04 mM of U(VI) in solution, respectively. The magnitude of the error bars in Fig. 1b demonstrates that the experiment with the lowest concentration of EDTA (0.5 mM EDTA) does not exhibit a significantly different reduction rate compared to the EDTA-free controls. Additionally, the 0.5 mM EDTA dataset in Fig. 1b appears to exhibit a significantly longer lag phase prior to significant reduction of U(VI), however the precise timing of this lag phase is difficult to constrain due to the experimental uncertainties coupled with the slow reduction rate of these experiments.

3.2. Results of U(VI) reduction experiments with Ca

The presence of dissolved Ca exerted an opposite effect to that of EDTA on the rate of U(VI) reduction (Fig. 2a and b). The experiment without dissolved Ca exhibited a steady decrease in total dissolved U concentration over the 5 h experiment, from an initial concentration of 0.49 mM to 0.24 mM after 5 h (Fig. 2a). In general, with increasing dissolved Ca concentration in the experiment, the rate of decrease in the concentration of total dissolved U slowed (Fig. 2a). The U(VI) concentrations in the Ca experiments exhibited a slower rate of reduction with increasing dissolved Ca concentrations (Fig. 2b). The experiment without dissolved Ca exhibited a steady decrease in U(VI) concentrations with time, and as in the EDTA experiments, the U(VI) concentrations in solution at any given time during the experiment were lower than the measured total dissolved U concentrations, likely due to the presence

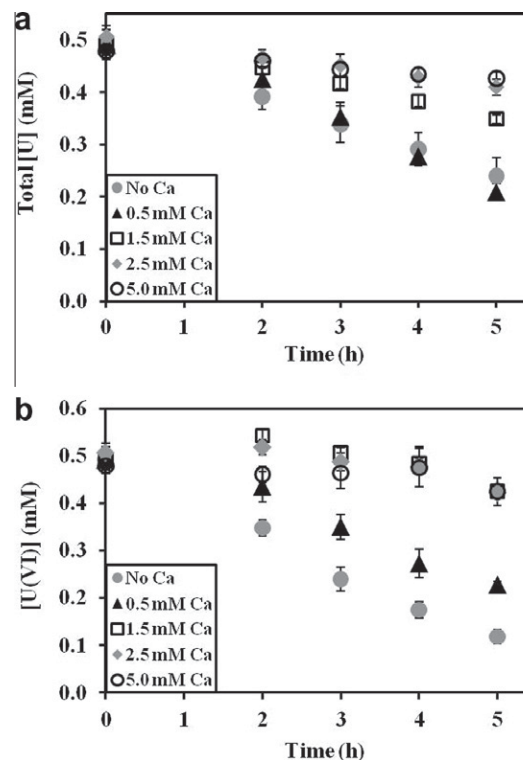


Fig. 2. The concentrations of (a) total dissolved U and (b) dissolved U(VI) remaining in solution in the presence of different concentrations of dissolved Ca (0.0, 0.5, 1.5, 2.5, and 5.0 mM) as a function of time. Symbols represent the average of triplicate experiments, and the error bars represent the associated standard deviation (1σ) of each value.

of UO₂ particles in the aqueous samples. The presence of Ca significantly slowed the rate of U(VI) reduction. For example, the concentrations of U(VI) in solution after 5 h in the 0, 0.5, and 5 mM Ca experiments were 0.12, 0.23, and 0.42 mM. Though our initial U(VI) concentration was much higher than that used by Brooks et al. (2003), our Ca experiments are consistent with their results in that the presence of dissolved Ca significantly slows the observed U(VI) bioreduction rate.

3.3. Results of U(VI) adsorption experiments

The results of our U(VI) adsorption experiment (Fig. 3) indicate that *S. oneidensis* exhibits similar U(VI) adsorption behavior as a function of pH to *B. subtilis* (Fowle et al., 2000; Gorman-Lewis et al., 2005). We observed extensive U(VI) adsorption onto *S. oneidensis* over the entire pH range studied (pH 3–9). The extent of U(VI) adsorption increased from pH 3 to 5, remained relatively constant from pH 5 to 6.5, and decreased slightly above pH 6.5. The percent of total U adsorbed onto the bacteria varied only between 29% and 75% in the presence of 0.25 g/L *S. oneidensis* and between 62% and 98% in the presence of 0.625 g/L *S. oneidensis* over the entire pH range studied. Increasing the bacterial concentration in the adsorption experiments from 0.25 to 0.625 g/L bacteria increased the

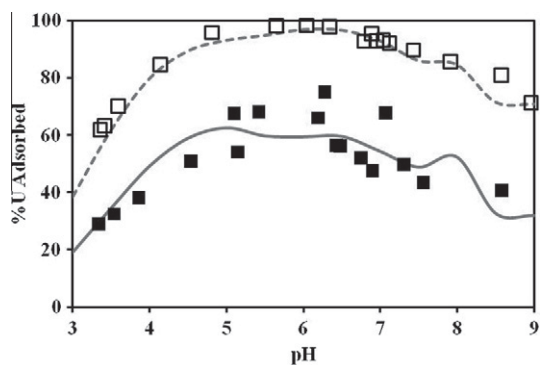


Fig. 3. Percentage of U(VI) adsorbed onto *S. oneidensis* MR-1 cells as a function of pH. Total concentration of U(VI) was 4.2×10^{-5} M; ionic strength was 0.1 M NaClO_4 . The open squares represent the experimental adsorption data for experiments with 0.625 g (wet mass)/L cells. The solid squares represent experimental adsorption data for experiments with 0.25 g (wet mass)/L cells. The dashed and solid curves represent predicted extents of U(VI) adsorption, calculated using the set of averaged K values listed in Table 1.

extent of U adsorbed onto the bacterial cells by approximately 30% across the pH range studied.

4. DISCUSSION

4.1. Effect of EDTA on the rate of U(VI) reduction

The addition of EDTA to the solutions in the U(VI) reduction experiments could cause two possible competing effects: (1) aqueous UO_2^{2+} -EDTA complexation could sequester U(VI) away from the bacteria in the system prior to reduction, causing a decrease in the rate of U(VI) reduction during the experiments; or (2) after U(VI) reduction to U(IV) on the cell wall, aqueous U^{4+} -EDTA complexation could draw U(IV) away from bacterial cell wall sites of reduction, speeding the reduction rate by freeing sites for more U(VI) to adsorb and become reduced. As pointed out by Haas and Northup (2004), the total dissolved U measurements do not distinguish between these two controls on the reduction rate as either mechanism would result in enhanced total dissolved U with increasing EDTA concentration. In the first case, the total dissolved U would be present as U(VI), and in the latter case, the aqueous U would be present as an aqueous U^{4+} -EDTA complex. However, the U(VI) measurements clearly demonstrate that EDTA increases the rate of U(VI) reduction in these systems, and that the reduction rate increases with increasing EDTA concentration. Our observations are consistent only with the formation of the aqueous U^{4+} -EDTA complex, which prevents the precipitation of UO_2 , and maintains virtually all of the U in solution. The results of this investigation also suggest that in the EDTA experiments the rate controlling step in the enzymatic reduction of U(VI) is not the adsorption or desorption rate of U(VI). If the U(VI) speciation controlled the reduction rate, then the reduction rate would decrease with increasing EDTA concentration due to the sequestration of U(VI) in solution by aqueous EDTA complexes. We observed the opposite

effect, which is best explained by aqueous U(IV)-EDTA complexation.

Our Ca experiments demonstrate an opposite effect to that of EDTA in that increasing concentrations of Ca in the experimental solutions decrease the rate of disappearance of both total dissolved U and aqueous U(VI). The most likely explanation for this observation is that the presence of Ca promotes the formation of aqueous Ca-uranyl-carbonate complexes and sequester U(VI) away from the bacterial cells. Although these complexes can adsorb onto the bacterial cell wall, the presence of Ca may decrease the net amount of adsorbed U(VI), sequestering U(VI) away from the cell wall, and thereby slowing U(VI) reduction. The effect of Ca on U(VI) reduction is opposite to that of EDTA: EDTA forms more stable complexes with U^{4+} than it does with UO_2^{2+} , so the presence of EDTA in the experiments affects the speciation of the reduction product more than it does the speciation of U(VI) in solution, and hence speeds reduction. Conversely, Ca does not affect U(IV) speciation or the solubility of UO_2 . Therefore, the addition of Ca to the experimental systems does not affect the removal rate of U(IV) from the cell wall or make reduction sites more available after the reduction of U(VI) to U(IV). However, increasing Ca concentration does affect the aqueous speciation of U(VI), promoting the formation of Ca-uranyl-carbonate aqueous complexes which sequester more U(VI) away from the bacterial cells. The decrease in U(VI) concentration on the cells with increasing Ca concentration appears to slow U(VI) reduction.

Our results suggest that the bacterial cell wall complexation of both U(VI) before reduction and U(IV) after reduction controls U(VI) reduction rates in our experimental systems. There have been no measurements of U^{4+} adsorption onto bacteria, so we can not quantify the effect of EDTA on the U(IV) speciation on the cell wall. However, as a proxy for models of U^{4+} speciation on the cell wall, we relate the U(VI) reduction rate in the EDTA experiments to the concentration of the aqueous U^{4+} -EDTA complex (Fig. 4). By assuming a pseudo-first-order reaction rate, we calculated the initial reduction rate (mM/h) of U(VI) as the decrease in aqueous U(VI) concentration versus time, defined by the slope of the best-fitting trendline of the dataset for each EDTA concentration in Fig. 1b. The concentration of the aqueous U^{4+} -EDTA complex was assumed to be the difference between the measured concentrations of total dissolved U and aqueous U(VI) for each EDTA concentration, and the data shown in Fig. 4 represent the concentrations of the U^{4+} -EDTA complex for each EDTA concentration at 2.3 h. The data from the experiments without EDTA were excluded from this treatment because most of the U(IV) that remained in the samples after filtration was likely present as UO_2 particles, whereas virtually all of the U(IV) in the EDTA-bearing systems was present as the aqueous U^{4+} -EDTA complex. Fig. 4 depicts a strong correlation between the U(VI) reduction rate and the concentration of the aqueous U^{4+} -EDTA complex at 2.3 h. Similar strong correlations exist between the reduction rate and the concentration of the U^{4+} -EDTA complex at the other sampling times (correlation not shown here). The strong relationship between the U(VI) reduction

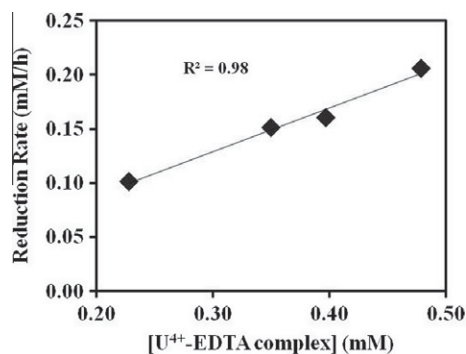


Fig. 4. Measured U(VI) reduction rates plotted as a function of the calculated concentration of the aqueous U⁴⁺-EDTA complex at the 2.3 h time point of the U(VI) reduction experiments with EDTA.

rate and the concentration of the aqueous U⁴⁺-EDTA complex supports our conclusion that EDTA controls the reduction rate by removing U⁴⁺ from reduction sites on the bacterial cell wall. Similarly, Suter et al. (1991) argued that the mineral surface release rate of Fe is the rate-controlling step in the reductive dissolution of Fe(III) (hydr)oxides. Our results also suggest that thermodynamic models of U(IV) speciation in realistic systems could yield reasonable predictions of the U(VI) reduction rates. U(VI) bioreduction rates are likely enhanced by ligands such as EDTA that preferentially bind with U(IV) relative to U(VI). For example, the presence of humic acid, which forms highly stable aqueous complexes with U(IV), also enhances the rate of U(VI) reduction by *S. oneidensis* (Gu et al., 2005) perhaps in part due to complexation effects.

4.2. Effect of Ca on the rate of U(VI) reduction

4.2.1. Quantifying U(VI) adsorption onto *S. oneidensis*

We use our U(VI) adsorption measurements to determine the speciation of U(VI) on *S. oneidensis* in order to determine if a relationship exists between cell wall uranyl speciation and U(VI) reduction rates in the U(VI) reduction experiments with Ca. We followed the modeling approach described by Gorman-Lewis et al. (2005) who measured U(VI) adsorption onto *B. subtilis* and used the results to determine the stability constants for the important U(VI)-bacterial surface complexes. Metal adsorption measurements conducted as a function of pH constrain the number of sites involved in metal binding, the pH range of influence, and the stability constants for the important

metal-bacterial surface complexes. We used the program FITEQL (Herbelin and Westall, 1994) for the equilibrium thermodynamic modeling of the U adsorption data, accounting for aqueous speciation using reactions 14–33 listed in electronic annex Table EA-1. Activity coefficients for ions were calculated within FITEQL using the Davies equation. A discrete pK_a 4-site non-electrostatic model was used to model the protonation behavior of the *S. oneidensis* cell wall functional groups (Mishra et al., 2010). We refer to Sites 1–4 as the sites with pK_a values of 3.3 ± 0.2, 4.8 ± 0.2, 6.7 ± 0.4, and 9.4 ± 0.5, respectively. The bacterial site density for each site was calculated according to the site densities of *S. oneidensis* described by Mishra et al. (2010), which are 8.9(±2.6) × 10⁻⁵, 1.3(±0.2) × 10⁻⁴, 5.9(±3.3) × 10⁻⁵ and 1.1(±0.6) × 10⁻⁴ mol per gram (wet mass) of *S. oneidensis* for sites 1–4, respectively. The adsorption experiments were conducted with the systems open to the atmosphere, so CO₂ in the aqueous systems was assumed to be in equilibrium with atmospheric CO₂.

We deconvolved the adsorption reactions that control U(VI) adsorption across the pH range studied by first modeling only the low pH (from pH 3 to 5) adsorption. Below pH 5, U is present in solution dominantly as the UO₂²⁺ cation, so the range of likely adsorption reactions is restricted. A model with UO₂²⁺ binding onto deprotonated Site 2 best fits the low pH data, with a reaction stoichiometry and calculated *K* value given in Table 1. Because of the diminished importance of UO₂²⁺ in the aqueous U budget above pH 5 and the increased importance of uranyl-hydroxide and -carbonate complexes, Reaction 1 from Table 1 cannot account for the observed extent of U(VI) adsorption from pH 5 to 7. Therefore, we fix the *K* value for Reaction 1 to our calculated value, and test a range of adsorption reactions involving binding of the important uranyl-hydroxide and -carbonate complexes onto deprotonated forms of Sites 2 and 3 to account for the mid-pH adsorption behavior, and using the V(Y) output of FITEQL to quantify model fits. Reaction 2 in Table 1 yields the best-fit to data in the mid-pH region; the inclusion of Reaction 3 in Table 1 is required in order to account for the observed extents of adsorption between pH 7 and 9. We modeled the 0.25 g/L and the 0.625 g/L U(VI) adsorption datasets separately, and both yielded best-fit models that include Reactions 1–3 in Table 1 (Fig. 3). The values listed for the stability constants for these reactions in Table 1 are the averages of the two datasets of stability constant values, which were calculated based on 0.25 g/L and 0.625 g/L adsorption data, respectively. The uncertainties listed in Table 1 were

Table 1
Uranyl surface complexation reactions for both *S. oneidensis* and *B. subtilis*.

		Log K (<i>S. oneidensis</i>)	Log K ^b (<i>B. subtilis</i>)
1	UO ₂ ²⁺ + R-L2 ^{-a} = R-L2-UO ₂ ⁺	6.2 ± 0.2	6.2 ± 0.3
2	UO ₂ (CO ₃) ⁰ + R-L2 ^{-a} = R-L2-UO ₂ CO ₃ ⁻	6.9 ± 0.3	5.5 ± 0.6
3	UO ₂ (CO ₃) ₃ ⁴⁻ + R-L3 ^{-a} = R-L3-UO ₂ (CO ₃) ₃ ⁵⁻	7.3 ± 0.2	7.3 ± 0.6

^a R-L#- represents *S. oneidensis* functional groups, Sites 1–4, with pK_a values of 3.3 ± 0.2, 4.8 ± 0.2, 6.7 ± 0.4, and 9.4 ± 0.5, respectively (Mishra et al., 2010).

^b Gorman-Lewis et al. (2005).

calculated by determining the range of K values that account for the observed range of experimental values for the extent of adsorption. The average K values for Reactions 1–3 were used to generate the model curves that are plotted in Fig. 3. The figure demonstrates that the set of average K values can account for the data well both as a function of pH and as a function of bacterial concentration.

The adsorption behavior that we observed for *S. oneidensis* is similar to that of *B. subtilis*. The log K values that we calculated for Reactions 1–3 for *S. oneidensis* are listed in Table 1, along with the corresponding log K values for *B. subtilis* reported by Gorman-Lewis et al. (2005). The calculated K values for Reactions 1 and 3 for *S. oneidensis* are in excellent agreement with corresponding K values for *B. subtilis*. The K values for Reaction 2 for these two bacterial species do not agree within uncertainties and may indicate enhanced adsorption by *S. oneidensis* under circumneutral pH conditions. The similarities in stability constants for Reactions 1 and 3 are consistent with the observations of similar Cd adsorption behavior and stability constants for a range of bacteria and bacterial consortia (Yee and Fein, 2001). Based on these similarities, we assumed that the stability constants for the important Ca–bacterial surface complexes for *S. oneidensis* (Reactions 1 and 2 in Table EA-1) are the same as those for *B. subtilis*, which were determined previously by Gorman-Lewis et al. (2005).

4.2.2. Relationship between U cell wall speciation and U(VI) reduction rate

The calculated stability constants for the uranyl–bacterial surface complexes enable calculation of the extent of U(VI) adsorption and the speciation of adsorbed U(VI) under the conditions of the U(VI) reduction experiments with Ca. These calculations enable tests of whether relationships exist between the observed reduction rates and the speciation of U(VI) on the bacterial cell wall in the Ca-bearing U(VI) reduction experiments. The initial reduction rates of U(VI) in the presence of different Ca concentrations were determined by calculating the slopes of the best-fitting trendlines of the data for each Ca concentration in Fig. 2b. The calculations of the U(VI) speciation in the systems of the U(VI) reduction experiments with Ca account for aqueous uranyl-hydroxide, -carbonate, -lactate, -acetate, and -bacterial surface complexation using the reactions and stability constants listed in Table 1 and Table EA-1. The system was also constrained with mass balance constraints on dissolved carbonate, lactate, acetate,

bacterial sites and U(VI) concentrations. Bacterial concentrations in the experiments were determined from the experimental suspensions, yielding an average experimental cell density of $3.2(\pm 0.6) \times 10^7$ cells/mL. This cell density was transformed into the wet mass density by dividing by a conversion factor of $1.9(\pm 0.6) \times 10^{10}$ cells/g, which was determined based on our cell mass–cell counts transformation experiments, in which cells of specific wet mass were counted by direct cell counting method after suspended in specific volume of solution. Bacterial site concentrations were calculated using *S. oneidensis* site densities reported by Mishra et al. (2010). The calculated total binding site concentration was 0.61 mM for the Ca experiments. The U(VI) speciation in the system without Ca was calculated in a similar way to the procedures described above, but excluding all Ca-bearing reactions in Table EA-1. The modeling results of the U(VI) reduction experiments with Ca indicate the presence and the concentrations of the important uranyl surface complexes, which are shown in Table 2.

We use our modeling results to test whether the observed reduction rates correlate with either the total concentration of adsorbed U(VI), the concentration of adsorbed Ca–uranyl–carbonate species, or the total concentration of adsorbed uranyl complexes that do not involve Ca. There is no consistent relationship between the total adsorbed U(VI) concentration and the U(VI) reduction rate. Fig. 5a depicts a strong negative correlation between the reduction rate and the concentration of the Ca–uranyl–carbonate surface complex (R-L2-Ca₂UO₂(CO₃)₃[−]). The strong negative correlation suggests that the U(VI) that is present as this species on the bacterial cell wall is not available for reduction, and the higher the concentration of U(VI) bound as R-L2-Ca₂UO₂(CO₃)₃[−], the slower the reduction rate. Conversely, Fig. 5b illustrates a strong positive correlation between the observed rate of U(VI) reduction in the Ca experiments and the sum of the concentrations of the Ca–free uranyl surface complexes (R-L2-UO₂⁺, R-L2-UO₂CO₃[−] and R-L3-UO₂(CO₃)₃^{5−}). The positive correlation shown in Fig. 5b strongly suggests that the only U(VI) that is available for reduction is the adsorbed U(VI) that exists on the cell wall as Ca–free uranyl surface complexes. Therefore, increasing the concentration of these Ca–free uranyl surface complexes also increases the rate of U(VI) reduction by *S. oneidensis* under the experimental conditions, and the concentration of these species on the bacterial cell wall is the primary control on the reduction rate.

Table 2
Calculated uranyl surface complexes formed in the Ca experiments.

[Ca] (mM)	Uranyl surface complexes (mM)				Total adsorbed U(VI)
	R-L2-UO ₂ ⁺ ^a	R-L2-UO ₂ CO ₃ [−] ^a	R-L3-UO ₂ (CO ₃) ₃ ^{5−a}	R-L2-Ca ₂ UO ₂ (CO ₃) ₃ ^{−a}	
0.0	3.1×10^{-7}	1.3×10^{-1}	1.0×10^{-1}	None	2.3×10^{-1}
0.5	1.2×10^{-7}	5.6×10^{-2}	1.0×10^{-1}	6.6×10^{-2}	2.2×10^{-1}
1.5	1.3×10^{-8}	6.1×10^{-3}	9.7×10^{-2}	1.6×10^{-1}	2.7×10^{-1}
2.5	4.6×10^{-9}	2.0×10^{-3}	8.8×10^{-2}	1.8×10^{-1}	2.7×10^{-1}
5.0	1.2×10^{-9}	4.8×10^{-4}	6.3×10^{-2}	1.9×10^{-1}	2.6×10^{-1}

^a R-L#- represents *S. oneidensis* functional groups, Sites 1–4, with pK_a values of 3.3 ± 0.2 , 4.8 ± 0.2 , 6.7 ± 0.4 , and 9.4 ± 0.5 , respectively (Mishra et al., 2010).

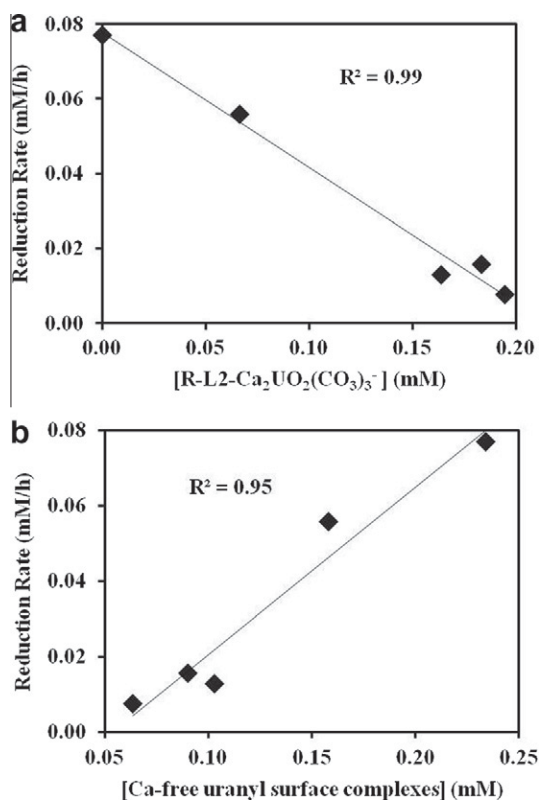


Fig. 5. (a) Measured U(VI) reduction rates plotted as a function of the concentration of the Ca-uranyl-carbonate bacterial surface complex (R-L2-Ca₂UO₂(CO₃)₃⁻). (b) Measured U(VI) reduction rates plotted as a function of the total concentration of the Ca-free uranyl surface complexes (R-L2-UO₂⁺, R-L2-UO₂CO₃⁻ and R-L3-UO₂(CO₃)₃²⁻).

We also considered the possibility that the Ca inhibition effect was due to competition for binding sites on the cell surface between U(VI) and Ca. Although the concentration of adsorbed Ca increases with increasing Ca in the experimental systems (modeling results not shown here), the surface sites are significantly undersaturated with bound Ca or U(VI), and our modeling results of the bacterial surface speciation (Table 2) indicate that the concentration of total U(VI) adsorbed onto the bacteria does not change significantly as a function of Ca concentration in the experiments. That is, the Ca concentration affects the speciation of surface-bound U(VI), but does not affect the total concentration of bound U(VI) through competitive adsorption.

5. CONCLUSIONS

Our experiments demonstrate that EDTA increases the rate of U(VI) reduction by *S. oneidensis* and that dissolved Ca decreases the reduction rate. In the EDTA-presenting U(VI) reduction systems, EDTA maintains all of the U in solution by forming U⁴⁺-EDTA complex after reduction of U(VI) to U(IV). Also there is a strong relationship between the U(VI) reduction rate and the concentration of the aqueous U⁴⁺-EDTA complex in the system. So we conclude that EDTA speeds U(VI) bioreduction by removing

U⁴⁺ from reduction sites on the bacterial cell wall. We measured uranyl adsorption onto *S. oneidensis* and use the results to search for relationships between the reduction rate and the speciation of U(VI) on the bacterial cell wall in the systems of U(VI) reduction experiments with Ca. We find that the reduction rate is negatively correlated with the concentration of R-L2-Ca₂UO₂(CO₃)₃⁻ suggesting that U(VI) cannot be reduced when present as the Ca-uranyl-carbonate complex on the bacterial cell wall. However, a strong positive correlation exists between the reduction rate and the concentration of uranyl-bacterial surface complexes that do not involve Ca. This finding suggests that U(VI) must be present on the cell wall as one of these complexes for reduction to occur, and the reduction rate is directly proportional to the concentration of these complexes on the cell wall.

The findings of this study could enable quantitative predictions of U(VI) reduction rates in realistic geologic systems. The presence of aqueous ligands such as EDTA which form significantly more stable aqueous complexes with U⁴⁺ than with UO₂²⁺ will increase the reduction rate of U(VI) by bacteria, and these ligands will also prevent the precipitation of UO₂ and help to maintain U dissolved in solution. Therefore, although the U(VI) reduction rate is increased, the mobility of U would be unaffected when strong complexing agents such as EDTA are present. A similar ligand effect may contribute to the enhancement of enzymatic Pu(IV) reduction by bacteria in the presence of NTA (Rusin et al., 1994). The results from our Ca experiments suggest that the rate of enzymatic U(VI) reduction is directly proportional to the concentration of Ca-free uranyl bacterial surface complexes, and that system components that prevent the formation of these surface complexes would slow the reduction rate. For example, the presence of mineral surfaces that adsorb UO₂²⁺ and thereby compete with the bacterial cell wall sites in binding UO₂²⁺ may significantly slow bacterial U(VI) reduction rate in field settings. Surface complexation modeling offers a means for accounting for these competitive effects, and the relationships derived here may apply to these more complex settings. The modeling approach outlined here can be used to calculate the speciation of U(VI) on the bacterial cell wall and thereby to predict the rate of enzymatic reduction of U(VI) to U(IV) by bacteria.

ACKNOWLEDGMENTS

This research was supported in part by a NSF Environmental Molecular Science Institute grant to University of Notre Dame (EAR02-21966). Some analyses were conducted using equipment in the Center for Environmental Science and Technology at University of Notre Dame. Three thorough journal reviews are appreciated and improved the presentation of the work significantly.

APPENDIX A. SUPPLEMENTARY DATA

Supplementary data associated with this article can be found, in the online version, at doi:10.1016/j.gca.2011.03.039.

REFERENCES

- Anderson R. T., Vronion H. A., Ortiz-Bernad I., Resch C. T., Long P. E., Dayvault R., Karp K., Marutzky S., Metzler D. R., Peacock A., White D. C., Lowe M. and Lovley D. R. (2003) Stimulating the in situ activity of *Geobacter* species to remove uranium from the groundwater of a uranium-contaminated aquifer. *Appl. Environ. Microbiol.* **69**, 5884–5891.
- Balch W. E. and Wolfe R. S. (1976) New approach to the cultivation of methanogenic bacteria: 2-mercaptoethanesulfonic acid (HS-CoM)-dependent growth of *Methanobacterium ruminantium* in a pressurized atmosphere. *Appl. Environ. Microbiol.* **32**, 781–791.
- Behrends T. and Van Cappellen P. (2005) Competition between enzymatic and abiotic reduction of uranium(VI) under iron reducing conditions. *Chem. Geol.* **220**, 315–327.
- Bonatti E., Fisher D. E., Joensuu O. and Rydell H. S. (1971) Postdepositional mobility of some transition elements, phosphorus, uranium and thorium in deep sea sediments. *Geochim. Cosmochim. Acta* **35**, 189–201.
- Borrok D., Turner B. F. and Fein J. B. (2005a) A universal surface complexation framework for modeling proton binding onto bacterial surfaces in the geological settings. *Am. J. Sci.* **305**, 826–853.
- Borrok D., Borrok M. J., Fein J. B. and Kiessling L. L. (2005b) Link between chemotactic response to Ni^{2+} and its adsorption onto the *Escherichia coli* cell surface. *Environ. Sci. Technol.* **39**, 5227–5233.
- Brina R. and Miller A. G. (1992) Direct detection of trace levels of uranium by laser-induced kinetic phosphorimetry. *Anal. Chem.* **64**, 1413–1418.
- Brooks S. C., Fredrickson J. K., Carroll S. L., Kennedy D. W., Zachara J. M., Plymale A. E., Kelly S. D., Kemner K. M. and Fendorf S. (2003) Inhibition of bacterial U(VI) reduction by calcium. *Environ. Sci. Technol.* **37**, 1850–1858.
- Fein J. B., Daughney C. J., Yee N. and Davis T. A. (1997) A chemical equilibrium model for metal adsorption onto bacterial surfaces. *Geochim. Cosmochim. Acta* **61**, 3319–3328.
- Finneran K. T., Anderson R. T., Nevin K. P. and Lovley D. R. (2002) Potential for bioremediation of uranium-contaminated aquifers with microbial U(VI) reduction. *Soil Sediment Contam.* **11**, 339–357.
- Fowle D. A. and Fein J. B. (2000) Experimental measurements of the reversibility of metal–bacteria adsorption reactions. *Chem. Geol.* **168**, 27–36.
- Fowle D. A., Fein J. B. and Martin A. M. (2000) Experimental study of uranyl adsorption onto *Bacillus subtilis*. *Environ. Sci. Technol.* **34**, 3737–3741.
- Gorby Y. A. and Lovley D. R. (1992) Enzymic uranium precipitation. *Environ. Sci. Technol.* **26**, 205–207.
- Gorman-Lewis D., Elias P. E. and Fein J. B. (2005) Adsorption of aqueous uranyl complexes onto *Bacillus subtilis* cells. *Environ. Sci. Technol.* **39**, 4906–4912.
- Gu B., Yan H., Zhou P. and Watson D. B. (2005) Natural humics impact uranium bioreduction and oxidation. *Environ. Sci. Technol.* **39**, 5268–5275.
- Haas J. R. and Northup A. (2004) Effects of aqueous complexation on reductive precipitation of uranium by *Shewanella putrefaciens*. *Geochem. Trans.* **5**, 41–48.
- Haas J. R., Dichristina T. J. and Wade R. (2001) Thermodynamics of U(VI) sorption onto *Shewanella putrefaciens*. *Chem. Geol.* **180**, 33–54.
- Herbelin A. and Westall J. C. (1994) FITEQL 3.1, A computer program for determination of chemical equilibrium constants from experimental data, Report 94-01. Department of Chemistry, Oregon State University, Corvallis, OR, USA.
- Kelly S. D., Kemner K. M., Fein J. B., Fowle D. A., Boyanov M. I., Bunker B. A. and Yee N. (2002) X-ray absorption fine structure determination of pH-dependent U-bacterial cell wall interactions. *Geochim. Cosmochim. Acta* **66**, 3855–3871.
- Langmuir D. (1997) *Aqueous Environmental Geochemistry*. Prentice Hall, New Jersey.
- Lovley D. R. and Phillips E. J. P. (1988) Novel mode of microbial energy metabolism: organic carbon oxidation coupled to dissimilatory reduction of iron or manganese. *Appl. Environ. Microbiol.* **54**, 1472–1480.
- Lovley D. R. and Phillips E. J. P. (1992a) Reduction of uranium by *Desulfovibrio desulfuricans*. *Appl. Environ. Microbiol.* **58**, 850–856.
- Lovley D. R. and Phillips E. J. P. (1992b) Bioremediation of uranium contamination with enzymatic uranium reduction. *Environ. Sci. Technol.* **26**, 2228–2234.
- Lovley D. R., Phillips E. J. P., Gorby Y. A. and Landa E. R. (1991) Microbial reduction of uranium. *Nature* **350**, 413–416.
- Lovley D. R., Rodena E. E., Phillips E. J. P. and Woodward J. C. (1993) Enzymatic iron and uranium reduction by sulfate-reducing bacteria. *Marine Geol.* **113**, 41–53.
- Mishra B., Boyanov M., Bunker B. A., Kelly S. D., Kemner K. M. and Fein J. B. (2010) High- and low-affinity binding sites for Cd on the bacterial cell walls of *Bacillus subtilis* and *Shewanella oneidensis*. *Geochim. Cosmochim. Acta* **74**, 4219–4233.
- Neiss J., Stewart B. D., Nico P. S. and Fendorf S. (2007) Speciation-dependent microbial reduction of uranium within iron-coated sands. *Environ. Sci. Technol.* **41**, 7343–7348.
- Rusin P. A., Quintana L., Brainard J. R., Strietelmeier B. A., Tait C. D., Ekberg S. A., Palmer P. D., Newton T. W. and Clark D. L. (1994) Solubilization of plutonium hydrous oxide by iron-reducing bacteria. *Environ. Sci. Technol.* **28**, 1686–1690.
- Sill C. W. and Peterson H. E. (1947) Fluorescence test for uranium in aqueous solution. *Anal. Chem.* **19**, 646–651.
- Suter D., Banwart S. and Stumm W. (1991) dissolution of hydrous iron(III) oxides by reductive mechanisms. *Langmuir* **7**, 809–813.
- Stewart B. D., Neiss J. and Fendorf S. (2007) quantifying constraints imposed by calcium and iron on bacterial reduction of Uranium(VI). *J. Environ. Qual.* **36**, 363–372.
- Suzuki Y., Tanaka K., Kozai N. and Ohnuki T. (2010) Effects of Citrate, NTA, and EDTA on the reduction of U(VI) by *Shewanella putrefaciens*. *Geomicrobiol. J.* **27**, 245–250.
- Wu W. M., Carley J., Luo J., Ginder-Vogel M. A., Cardenas E., Leigh M. B., Hwang C., Kelly S. D., Ruan C., Wu L., Nostrand J. V., Gentry T., Lowe K., Mehlhorn T., Carroll S., Luo W., Fields M. W., Gu B., Watson D., Kemner K. M., Marsh T., Tiedje J., Zhou J., Fendorf S., Kitanidis P. K., Jardine P. M. and Criddle C. S. (2007) In Situ bioreduction of Uranium (VI) to submicromolar levels and reoxidation by dissolved oxygen. *Environ. Sci. Technol.* **41**, 5716–5723.
- Yee N. and Fein J. (2001) Cd adsorption onto bacterial surfaces: a universal adsorption edge? *Geochim. Cosmochim. Acta* **65**, 2037–2042.

Associate editor: Johnson R. Haas